Multi-band microwave metamaterial absorber based on coplanar Jerusalem crosses*

Wang Guo-Dong(王国栋)[a], Liu Ming-Hai(刘明海)[a)†], Hu Xi-Wei(胡希伟)[a)b)], Kong Ling-Hua(孔令华)[a], Cheng Li-Li(程莉莉)[b], and Chen Zhao-Quan(陈兆权)[c)]

[a)] *State Key Laboratory of Advanced Electromagnetic Engineering and Technology, Huazhong University of Science and Technology, Wuhan* 430074, *China*
[b)] *School of Physics, Huazhong University of Science and Technology, Wuhan* 430074, *China*
[c)] *College of Electrical and Information Engineering, Anhui University of Science and Technology, Huainan* 232001, *China*

(Received 3 April 2013; revised manuscript received 28 May 2013; published 3 December 2013)

The influence of the gap on the absorption performance of the conventional split ring resonator (SRR) absorber is investigated at microwave frequencies. Our simulated results reveal that the geometry of the square SRR can be equivalent to a Jerusalem cross (JC) resonator and its corresponding metamaterial absorber (MA) is changed to a JC absorber. The JC MA exhibits an experimental absorption peak of 99.1% at 8.72 GHz, which shows an excellent agreement with our simulated results. By simply assembling several JCs with slightly different geometric parameters next to each other into a unit cell, a perfect multi-band absorption can be effectively obtained. The experimental results show that the MA has four distinct and strong absorption peaks at 8.32 GHz, 9.8 GHz, 11.52 GHz and 13.24 GHz. Finally, the multi-reflection interference theory is introduced to interpret the absorption mechanism.

Keywords: Jerusalem cross, multi-band metamaterial absorber, multi-reflection interference theory

PACS: 78.20.Ci, 42.25.Bs, 41.20.Jb **DOI:** 10.1088/1674-1056/23/1/017802

1. Introduction

Recently, the design of an electromagnetic (EM) metamaterial absorber (MA) with nearly unity absorption has attracted enormous research interest. The seminal work of the ultrathin MA was firstly proposed by Bilotti *et al*. in the microwave region. That absorber consisted of an array of split ring resonators (SRRs) and a resistive sheet to absorb the EM energy of the incident wave at the resonance frequency.[1] In 2008, Landy *et al*. experimentally demonstrated a thin perfect MA at 11.5 GHz, which was made of a sub-wavelength structure of electric ring resonators and metal cut wires separated by a dielectric substrate.[2] By manipulating the electric and magnetic resonances independently, it is possible to achieve $\varepsilon = \mu$, matching the impedance to the free space, and attain a large imaginary part in the refraction index n_2 simultaneously. Both the reflection and transmission waves are minimized at the same frequency and hence the absorption is maximized with the incident energy being converted into heat.

Compared to the conventional microwave absorber, the MA has several unparalleled advantages. First, it can flexibly manipulate the EM properties, which gives more flexible design options. Second, the thickness of the MA is significantly thinner than that of the conventional absorber which is restricted by the diffraction limit. Third, the design and fabrication of the MA are simple. However, the high absorption of the MA is generally based on electromagnetic resonances, so its working bandwidth is relatively narrow. In the past five years, most of the efforts were made on MAs to achieve polarization-insensitive absorption,[3–5] wide-angle absorption,[6–8] multi-band absorption[9,10] and broadband absorption.[11–13] To date, the MAs have been demonstrated in every technologically relevant spectral range, from the microwave region,[1–3,5,8,10,12] the terahertz region,[4,9,11,13] to the infrared region,[6,14] and even to the optical region.[7,15]

In this paper, we investigate the absorption rates of the SRR MA with various values of the gap and the I-shaped MA at microwave frequencies. The Jerusalem cross (JC) MA exhibits an experimental absorption peak of 99.1% at 8.72 GHz and could work at wide angles of incidence for both transverse electric (TE) and transverse magnetic (TM) waves. Importantly, the perfect multi-band absorption can be obtained by simply assembling several JCs with slightly different parameters into a unit cell. The fabricated MA has four distinct absorption peaks at 8.32 GHz, 9.8 GHz, 11.52 GHz and 13.24 GHz with absorption rates of 96.2%, 96.7%, 99.5% and 99.1%, respectively. We adopt a new physical mechanism to explain the absorption. The calculated absorption spectra using the interference model agree well with the simulated and experimental results.

*Project supported by the National Natural Science Foundation of China (Grant Nos. 10775055 and 11105002) and the Open-end Fund of State Key Laboratory of Structural Analysis for Industrial Equipment, China (Grant No. GZ1215).

†Corresponding author. E-mail: mhliu@mail.hust.edu.cn

© 2014 Chinese Physical Society and IOP Publishing Ltd

2. Designs and experiments of multi-band MA

2.1. Absorption of conventional SRR MA

The schematic diagram and geometric parameters of the SRR MA unit cell are illustrated in Fig. 1(a). The unit cell is composed of a metallic SRR and a continuous metal film separated by a dielectric substrate. The top square SRR strongly couples to the incident electric field and exhibits a pure electric response as counter-circulating currents in the unit cell eliminate any magnetoelectric response.[16] The incident magnetic field couples to two metallic layers on both sides of the dielectric substrate, which exhibits a magnetic resonance.[2,11] We can obtain tailored electric and magnetic resonances at the same frequency by tuning the geometric parameters of the unit cell and achieve a perfect absorption.

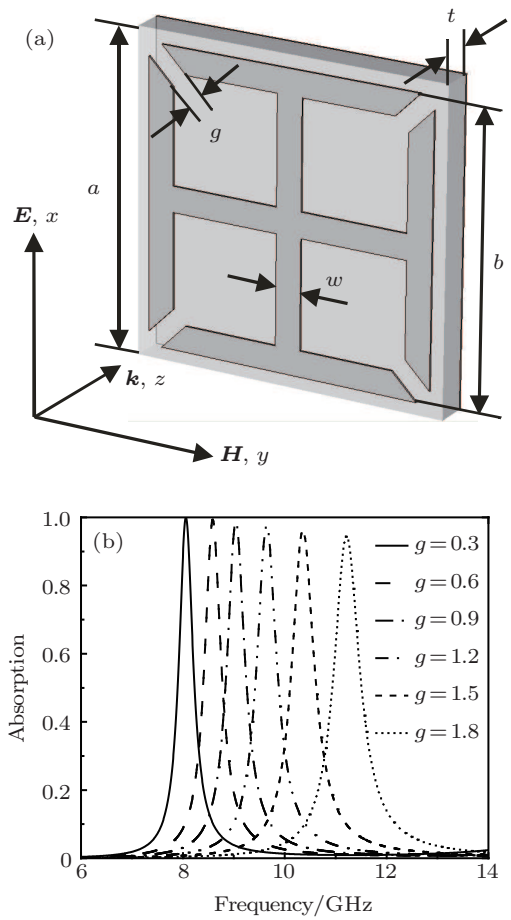


Fig. 1. (a) Schematic diagram and geometric parameters of the SRR MA unit cell with axes indicating the polarization and propagation directions of the incident wave. (b) Simulated absorption rates of the SRR MA with various values of the gap.

The proposed MA is designed and optimized based on the commercial finite difference time domain (FDTD) solver Microwave Studio by CST. The periodic boundary condition is set along the lateral directions of the structure and the open boundary condition is set along the z direction. A frequency domain solver and a hexahedral mesh are used in our design. A lossy FR-4 substrate with relative permittivity $\varepsilon_r = 4.3$ and loss tangent $\tan\delta = 0.025$ is used in the MA. The metallic material is copper with electric conductivity $\sigma = 5.8 \times 10^7$ S/m. The final optimized geometry of the unit cell has $a = 5$ mm, $b = 4.6$ mm, $w = 0.4$ mm and $t = 0.5$ mm. The transmission is zero in the whole frequency range due to the shielding of the copper film; the reflection is the only factor determining the absorption. Therefore, the absorption rate is calculated by $A(w) = 1 - R(w) = 1 - |S_{11}|^2$.[10]

The absorption rates of the SRR MA with various values of the gap are shown in Fig. 1(b). An absorption peak of 99.9% is obtained at the frequency of 8.06 GHz when the gap is $g = 0.3$ mm. As the gap increases, the absorption peak decreases slightly, however, the resonance frequency shifts to the blue region significantly. When the gap increases to $g = 1.8$ mm, the absorption peak achieves 94.6% at 11.22 GHz. These results indicate that the gap affects the absorption of the MA insignificantly but it affects the resonance frequency significantly.

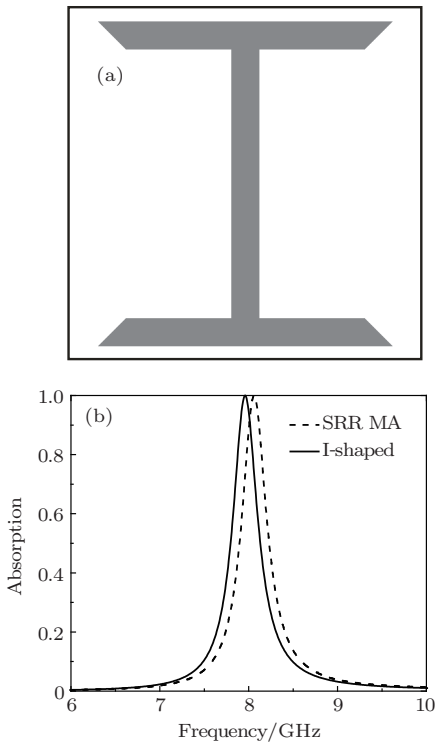


Fig. 2. (a) Schematic diagram of the I-shaped MA unit cell. (b) Simulated absorption rates of the SRR MA ($g = 0.3$ mm) and the I-shaped MA.

To understand where the absorption of the SRR MA occurs, the I-shaped MA with the same parameters as those of the vertical half of the SRR MA ($g = 0.3$ mm) is simulated. The polarization and propagation directions of the incident wave remain unchanged. The unit cell of the I-shaped MA and its corresponding absorption rate are given in Figs. 2(a) and 2(b), respectively. The absorption rate of the SRR MA is also shown in Fig. 2(b) as a reference. It is easily seen that the I-shaped

MA exhibits an absorption peak at 7.96 GHz with an absorption rate of 99.9%. This peak agrees well with that of the SRR MA with a 100 MHz redshift, which can be explained by the lack of the horizontal I-shaped resonator on the top layer. Similar to the MA composed of two sets of I-shaped resonators, the resonance frequency of the absorption is primarily determined by the length of the end loading.[13] We conclude that the absorption mainly depends on the vertical I-shaped structure at normal incidence and therefore the SRR structure can be regarded as crossed I-shaped resonators.

2.2. Design and experiment of single-band MA

Based on the above discussion, the geometry of the conventional square SRR can be simplified as a JC structure and thus its corresponding MA is changed to a JC absorber. The JC resonator has been proposed in constructing three-dimensional metamaterials by Wang *et al*. and is polarization-insensitive because of its fourfold rotational symmetry about the propagation axis.[17,18] Figure 3(a) depicts the simplified JC MA unit cell, which consists of a JC resonator, a dielectric substrate and a continuous copper film. The geometric parameters of the JC MA are the same as those of the SRR MA except for $l = 3.4$ mm. The simulated absorption rate of the JC MA is shown in Fig. 3(c). We can easily see that an absorption peak at the frequency of 8.69 GHz with an absorption rate of over 97.6% is obtained.

The JC MA was fabricated into a 180 mm×180 mm sample by printed circuit board (PCB) technology, as shown in Fig. 3(b). The MA sample was characterized through free space reflection measurements in a microwave anechoic chamber. An Agilent N5244A vector network analyzer and two broadband horn antennas were connected by a coaxial cable. Two antennas were used to emit and receive the electromagnetic wave. Many pyramid absorbing materials were placed around the MA sample to eliminate the electromagnetic interference from the surrounding environment. The distance between the sample and the antennas was set at about 2.5 m to avoid the near-field effect. A bare aluminum board with the same sizes as the sample was used as a calibration. The ratio of the reflectance between the sample and the aluminum board was regarded as the reflectance of the MA. As shown in Fig. 3(c), the fabricated MA exhibits a perfect experimental absorption peak at 8.72 GHz, which shows an excellent agreement with the simulated results.

The absorption rates of the JC MA at different angles of incidence for TE and TM waves are depicted in Fig. 4. For the TE wave (see Fig. 4(a)), the absorption peak of 99.4% is achieved at the normal incidence. With the increasing angle of incidence, the peak slightly decreases and has an absorption rate of 92.6% at an incidence angle of 60°. When the incident angle further increases, the peak suddenly decreases, as the y component of the incident magnetic field becomes smaller and smaller and can no longer effectively induce a strong magnetic resonance. For the case of the TM wave (see Fig. 4(b)), the absorption spectra almost remain the same except that the resonance frequency has a small blue shift as the incident angle increases. This is because the direction of the incident magnetic field remains unchanged at different angles of incidence and it can efficiently drive a strong magnetic resonance. These results demonstrate that the JC MA could achieve a high absorption at wide angles of incidence for both TE and TM waves.

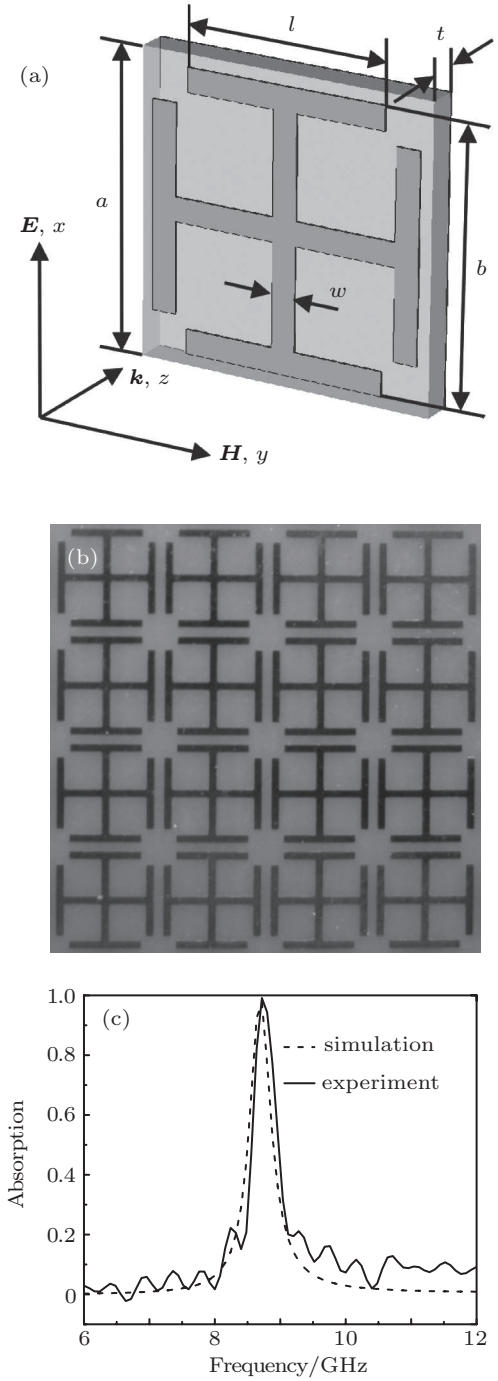


Fig. 3. (a) Schematic diagram and geometric parameters of the JC MA unit cell. (b) Photograph of a portion of the fabricated JC absorber. (c) Simulated and experimental absorption rates of the JC MA.

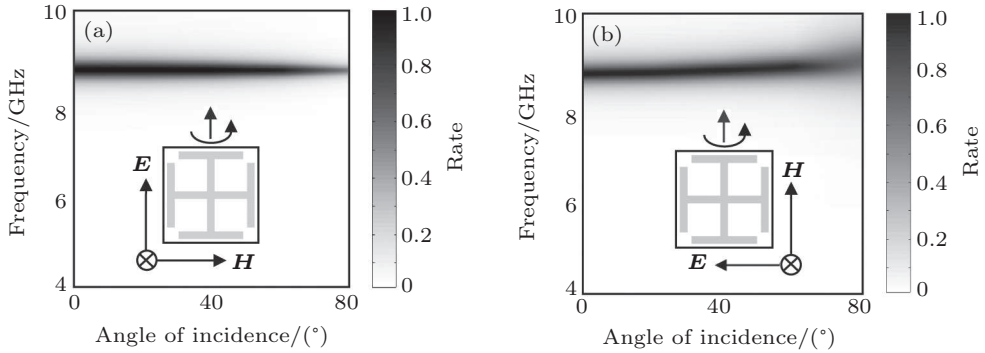


Fig. 4. Absorption rates of the JC MA at different angles of incidence for (a) TE and (b) TM waves. The insets indicate the polarization and propagation directions of the incident wave.

2.3. Design and experiment of multi-band MA

Based on the JC MA, we assemble several JCs with slightly different geometric parameters next to each other into a unit cell to achieve a multi-band absorber.[12,19] Figure 5(a) illustrates the schematic diagram of the four-band MA unit cell. The final parameters of the unit cell are given by $a =$ 5 mm, $b_1 = 4.6$ mm, $b_2 = 4.3$ mm, $b_3 = 3.9$ mm, $b_4 = 3.6$ mm, $l_1 = 3.4$ mm, $l_2 = 3$ mm, $l_3 = 2.6$ mm, $l_4 = 2.2$ mm, $c = 20$ mm and $w = 0.4$ mm. The four-band structure was fabricated into a 200 mm×200 mm sample as shown in Fig. 5(b). Figure 5(c) illustrates the simulated and experimental absorption rates of the four-band MA. It is easily seen that the fabricated MA has four distinct absorption peaks at 8.32 GHz, 9.8 GHz, 11.52 GHz and 13.24 GHz with the corresponding absorption rates of 96.2%, 96.7%, 99.5% and 99.1%. The simulated and experimental results are in good agreement except for a 200 MHz frequency red shift in the third resonance, which may be caused by fabrication inaccuracy and measurement errors.

The simulated power-loss density distributions in the four-band MA are displayed in Fig. 6, where Figs. 6(a)–6(d) respectively show the power loss distributions of the incident wave at 8.24 GHz, 9.8 GHz, 11.72 GHz and 13.24 GHz. In Fig. 6, each distribution of the power-loss density corresponds to a resonance frequency. Most of the power loss takes place in the upper and lower parts of the JC structure and the dielectric losses occur in between the two metallic layers where the

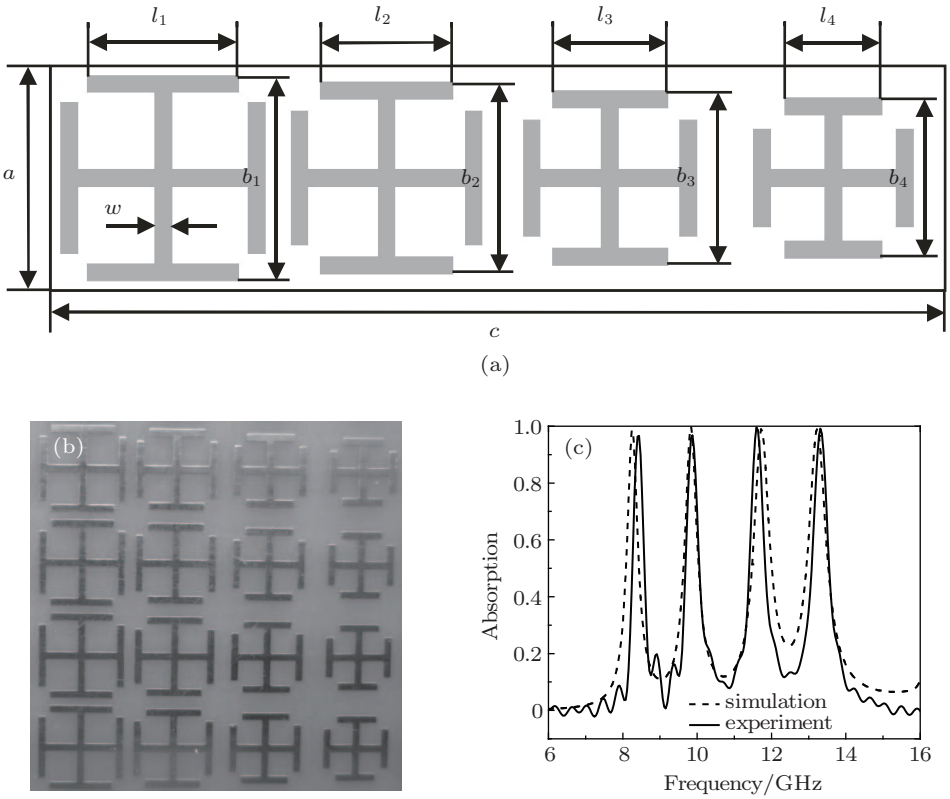


Fig. 5. (a) Schematic diagram and geometric parameters of the four-band MA unit cell. (b) Photograph of a portion of the fabricated four-band absorber. (c) Simulated and experimental absorption rates of the four-band MA.

EM field is very large.[2,19] The larger-size JCs correspond to a lower-frequency resonance, while the smaller-size JCs correspond to a higher-frequency resonance. These resonance characteristics are similar to those of the cut wires and square patch structures.[11,12] Therefore, the MA with four JCs of slightly different parameters can achieve a perfect four-band absorption.

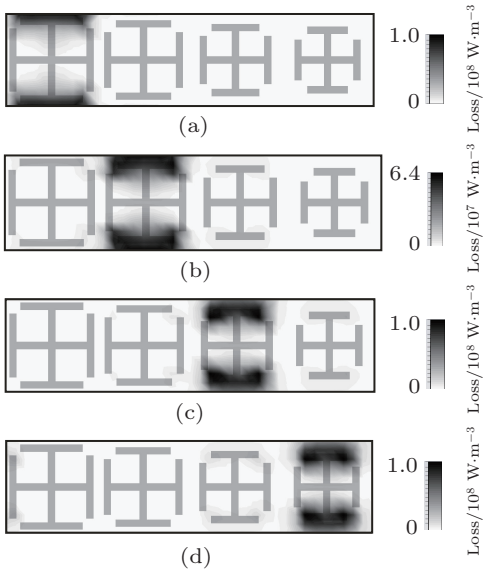


Fig. 6. Distributions of the power-loss density in the four-band MA at the resonance frequencies of (a) 8.24 GHz, (b) 9.8 GHz, (c) 11.72 GHz and (d) 13.24 GHz.

3. Multi-reflection interference theory

Different absorption mechanisms of the MA have been proposed in the previous papers.[20,21] The generally accepted impedance matching model can only qualitatively analyze the absorption. Here, we adopt the interference theory to analyze the absorption of the MA quantitatively. For simplicity, we take the JC MA for example. As shown in Fig. 7, the system contains two interfaces, the JC layer and the copper film. The JC resonator acts as a part of the reflection surface that can reflect/transmit a part of the incident wave. The copper film works as a perfect reflector with a reflectance of -1, thus the transmission through the MA is zero. The overall reflection is the superposition of the multiple reflections at the JC interface

$$\widetilde{r} = \frac{\widetilde{r}_{12} - \widetilde{\alpha}\,\mathrm{e}^{2\mathrm{i}\widetilde{\beta}}}{1 + \widetilde{r}_{21}\,\mathrm{e}^{2\mathrm{i}\widetilde{\beta}}}, \tag{1}$$

where $\widetilde{r}_{12}, \widetilde{r}_{21}, \widetilde{t}_{12}$ and $\widetilde{t}_{21}$ are the reflection and transmission coefficients of the JC interface, $\widetilde{\beta} = \sqrt{\widetilde{\varepsilon}} k_0 t$ is the propagation phase in the spacer, k_0 is the free space wavenumber and $\widetilde{\alpha} = \widetilde{t}_{12}\widetilde{t}_{21} - \widetilde{r}_{12}\widetilde{r}_{21}$.

To attain a nearly unity absorption at the resonance frequency, i.e., the reflectance is almost zero, the overall reflection coefficient should satisfy the following conditions:

$$|\widetilde{r}_{12}| = |\widetilde{\alpha}|, \tag{2}$$

$$\varphi(\widetilde{r}_{12}) - \varphi(\widetilde{\alpha}) - 2\beta = 2n\pi, \quad |n| = 0, 1, 2, \ldots. \tag{3}$$

To examine the above conditions, we simulate an isolated JC

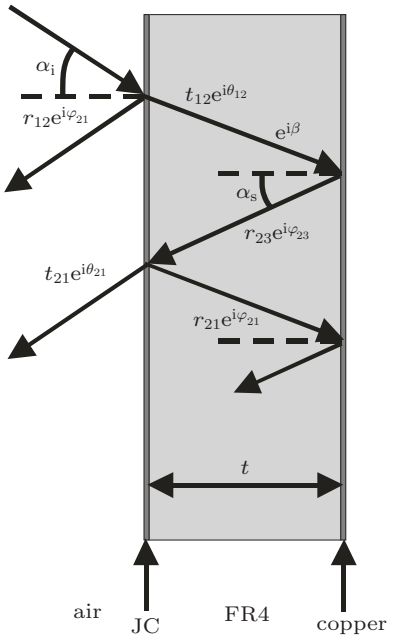


Fig. 7. The interference model of the JC MA and associated variables.

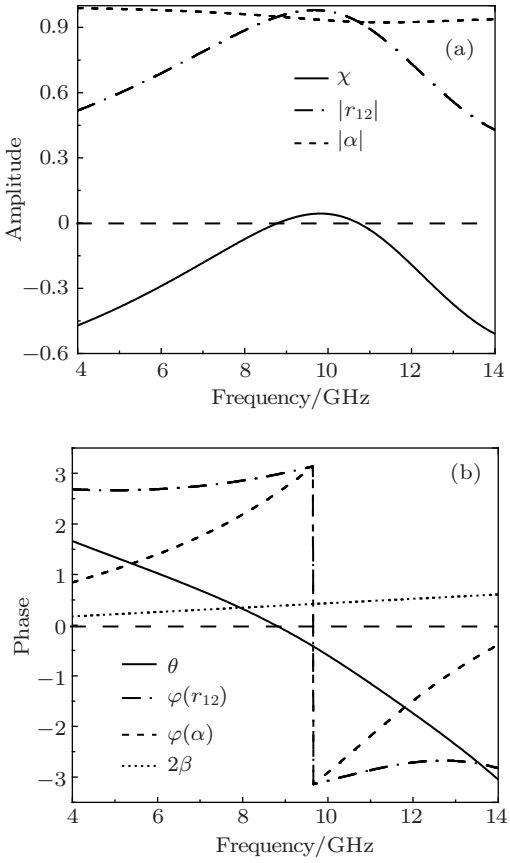


Fig. 8. (a) Amplitude $\chi = |\widetilde{r}_{12}| - |\widetilde{\alpha}|$ and the amplitudes of $\widetilde{r}_{12}$ and $\widetilde{\alpha}$; (b) phase $\theta = \varphi(\widetilde{r}_{12}) - \varphi(\widetilde{\alpha}) - 2\beta - 2n\pi$, the phases of $\widetilde{r}_{12}$ and $\widetilde{\alpha}$, and the propagation phase 2β obtained by numerical simulations using the unit cell shown in Fig. 3(a) for the decoupled model. For simplicity, the tildes on the top of r_{12} and α are neglected in the figures.

layer by Microwave Studio. For the JC interface, the copper film is removed and the thicknesses of air and substrate are set to 4 mm. As depicted in Fig. 8(a), at the frequency of 8.77 GHz, the amplitude is almost $\chi = 0$, where the amplitudes of $\widetilde{r}_{12}$ and $\widetilde{\alpha}$ are equal, satisfying the amplitude condition (2). From Fig. 8(b), the phase is $\theta = 0$ at 8.77 GHz, which perfectly fulfills the phase condition (3). The amplitude and phase conditions are simultaneously satisfied at 8.77 GHz and hence a perfect absorption is achieved. The calculated reflectance and absorption rates of the MA using the interference model are illustrated in Fig. 9. At the frequency of 8.77 GHz, an obvious dip appears in the reflectance spectrum and the corresponding absorption rate achieves 99.9%. The calculated absorption spectra using the interference model agree well with the simulated and experimental results given in Fig. 3(c). As a result, this method provides a rational physical insight into the absorption mechanism.

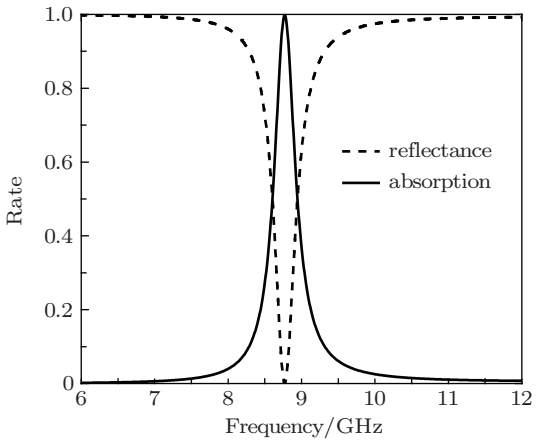


Fig. 9. Calculated reflectance and absorption rates of the JC MA using the interference model.

4. Conclusion

In conclusion, we investigate the absorption rates of the SRR MA with various values of the gap and the I-shaped MA at microwave frequencies. Our simulated results reveal that the geometry of the conventional SRR can be simplified as a JC resonator and thus the SRR MA is changed to a JC absorber. The JC MA exhibits an experimental absorption peak of 99.1% at 8.72 GHz and could operate well at wide angles of incidence for both TE and TM waves. Moreover, we have successfully demonstrated that a multi-band absorption can be effectively obtained by assembling several JCs with slightly different geometric parameters next to each other into a unit cell. The experimental results show that the MA has four distinct absorption peaks at 8.32 GHz, 9.8 GHz, 11.52 GHz and 13.24 GHz with the corresponding absorption rates of 96.2%, 96.7%, 99.5% and 99.1%. Finally, the multi-reflection interference theory is introduced to explain the absorption mechanism. The calculated absorption spectra using the interference model agree well with the simulated and experimental results. This proposed multi-band MA has many potential applications, such as the spectroscopic detection and phase imaging of hazardous materials and prohibited drugs, which require distinct absorption features at multiple frequencies.

References

[1] Bilotti F, Nucci L and Vegni L 2006 *Microw. Opt. Techn. Lett.* **48** 2171
[2] Landy N I, Sajuyigbe S, Mock J J, Smith D R and Padilla W J 2008 *Phys. Rev. Lett.* **100** 207402
[3] Gu C, Qu S B, Pei Z B and Xu Z 2011 *Chin. Phys. B* **20** 037801
[4] Landy N I, Bingham C M, Tyler T, Jokerst N, Smith D R and Padilla W J 2009 *Phys. Rev. B* **79** 125104
[5] Zhu W R, Zhao X P, Bao S and Zhang Y P 2010 *Chin. Phys. Lett.* **27** 014204
[6] Zhu W R and Zhao X P 2009 *J. Opt. Soc. Am. B* **26** 2382
[7] Zhu W R, Zhao X P, Gong B Y, Liu L H and Su B 2011 *Appl. Phys. A Mater.* **102** 147
[8] Zhu B, Wang Z B, Yu Z Z, Zhang Q, Zhao J M, Feng Y J and Jiang T 2009 *Chin. Phys. Lett.* **26** 114102
[9] Gu C, Qu S B, Pei Z B, Xu Z, Liu J and Gu W 2011 *Chin. Phys. B* **20** 017801
[10] Li H, Yuan L H, Zhou B, Shen X P, Cheng Q and Cui T J 2011 *J. Appl. Phys.* **110** 014909
[11] Ye Y Q, Jin Y and He S L 2010 *J. Opt. Soc. Am. B* **27** 498
[12] Luo H, Cheng Y Z and Gong R Z 2011 *Eur. Phys. J. B* **81** 387
[13] Huang L, Chowdhury D R, Ramani S, Reiten M T, Luo S N, Taylor A J and Chen H T 2012 *Opt. Lett.* **37** 154
[14] Jiang Z H, Yun S, Toor F, Werner D H and Mayer T S 2011 *ACS Nano* **5** 4641
[15] Hu C G, Liu L Y, Zhao Z Y, Chen X N and Luo X G 2009 *Opt. Express* **17** 16745
[16] Padilla W J, Aronsson M T, Highstrete C, Lee M, Taylor A J and Averitt R D 2007 *Phys. Rev. B* **75** 041102
[17] Wang J F, Qu S B, Xu Z, Fu Xu Z T, Ma H and Yang Y M 2009 *J. Phys. D: Appl. Phys.* **42** 155413
[18] Wang J F, Qu S B, Ma H, Xia S, Yang Y M, Lu L, Wu X, Xu Z and Wang Q 2010 *Piers Online* **6** 31
[19] Cheng Y Z, Nie Y, Gong R Z and Yang H L 2011 *Eur. Phys. J. Appl. Phys.* **56** 31301
[20] Smith D R, Vier D C, Koschny Th and Soukoulis C M 2005 *Phys. Rev. B* **71** 036617
[21] Chen H T 2012 *Opt. Express* **20** 7165